

# Multifunctional super-aligned carbon nanotube/polyimide composite film heaters and actuators



Wen Ning<sup>a,1</sup>, Zhenhe Wang<sup>b,1</sup>, Peng Liu<sup>a,\*</sup>, Duanliang Zhou<sup>a</sup>, Shiyong Yang<sup>b,\*\*\*</sup>,  
Jiaping Wang<sup>a</sup>, Qunqing Li<sup>a</sup>, Shoushan Fan<sup>a</sup>, Kaili Jiang<sup>a,\*\*</sup>

<sup>a</sup> State Key Laboratory of Low-Dimensional Quantum Physics, Department of Physics & Tsinghua-Foxconn Nanotechnology Research Center, Tsinghua University & Collaborative Innovation Center of Quantum Matter, Beijing, 100084, China

<sup>b</sup> Laboratory of Advanced Polymer Materials, Institute of Chemistry, Chinese Academy of Sciences, Beijing, 100190, China

## ARTICLE INFO

### Article history:

Received 6 March 2018

Received in revised form

24 July 2018

Accepted 2 August 2018

Available online 9 August 2018

## ABSTRACT

Polyimide (PI) is a high-performance polymer with ultrahigh heat stability while carbon nanotube (CNT) possesses high mechanical strength, excellent electrical and thermal conductivity. Here we report a facile and low-cost method free from CNT pre-dispersion for fabricating super-aligned carbon nanotube (SACNT)/PI composite film which combines the advantages of both SACNT and PI. Flexible and scratch-resistant composite film with high CNT content, uniform dispersion of CNTs, and controlled patterned CNT structures can be fabricated easily via in situ imidization. The SACNT/PI composite film exhibits improvement in mechanical strength, Young's modulus, electrical conductivity compared with pristine PI, and shows good thermal stability. Thanks to these superb properties, a flexible, stable, addressable, electromagnetic wave permeable, and high-temperature fast-response multifunctional heater as well as a thermo-mechanical actuator based on SACNT/PI composite film have been demonstrated in this paper. And it also shows great potential in a variety of applications such as flexible/wearable electronics, RFID, other thermo-related devices and so on.

© 2018 Elsevier Ltd. All rights reserved.

## 1. Introduction

Carbon nanotube (CNT) has been stimulating great interests since the report by Sumio Iijima in 1991 [1]. Because of its unique physical properties such as flexibility, light weight, high mechanical strength, excellent electrical and thermal conductivity, CNT is believed to be an ideal material to improve the performance of polymers [2–5]. Among the diverse polymer materials, polyimide (PI) possesses ultrahigh thermal stability (with a glass transition temperature ranging from 248 °C to 446 °C), resistance to radiation and solvent, as well as excellent mechanical and dielectric properties [6–9]. It has been found that the CNT/PI film's properties can be improved by combining the extraordinary properties of CNT and PI together. For instance, 5 wt% of CNTs can improve the electrical

conductivity of CNT/PI composite by 12 orders of magnitude [10], and the tensile strength by 40% compared with pristine PI [11]. The combination of high mechanical strength, ultrahigh flexibility, light weight, high thermal stability, and good electrical conductivity can meet the demands of applications in many fields ranging from microelectronics to aeronautics and astronautics.

A variety of methods for CNT/polymer composites have been developed including solution blending [12–16], melt blending [17,18] and buckypaper polymerization [19,20]. These traditional methods require pre-dispersion of CNTs in which case CNT content and dispersion uniformity are limited due to the large viscosity of resin, which restricts the performance of composites and increases the complexity of fabrication process. Based on the solution blending method, efforts have been made to improve the fabrication process. Dual-material aerosol jet printing method was developed to fabricate smart nanocomposite with tailorable and controllable intra-part varying CNT loading [21]. Inkjet printing method (directly printing the carbon nanotube polyimide suspension on a flexible polyimide substrate) was used to generate patterned electrical conductive nanocomposite thin films [22]. A three-dimensional porous PI/CNT composite aerogels were formed

\* Corresponding author.

\*\* Corresponding author.

\*\*\* Corresponding author.

E-mail addresses: [pengliu@tsinghua.edu.cn](mailto:pengliu@tsinghua.edu.cn) (P. Liu), [shiyang@iccas.ac.cn](mailto:shiyang@iccas.ac.cn) (S. Yang), [jiangkl@tsinghua.edu.cn](mailto:jiangkl@tsinghua.edu.cn) (K. Jiang).

<sup>1</sup> These authors contributed equally to this work.

by freeze-drying method [23]. These methods still need the pre-dispersion of CNTs and are not environmentally friendly. Therefore, it is still a challenge to simultaneously achieve high content, uniform dispersion, and orientation-controlled patterning of CNTs in composite films with a low-cost method. CNT/PI composites with high CNT fraction and high degree orientation were fabricated by infiltration-winding method [24]. Super-aligned CNT (SACNT) film is ultrathin, transparent, flexible, stretchable, and highly conductive, which is a suitable candidate for fabricating composite since the CNTs are parallel-aligned and uniformly distributed in it [25–27]. Moreover, the SACNT film can be patterned simply by laser cutting [28], which enables flexible and scratch-resistant composite films with controlled patterned CNT structures.

Here we report a facile and low-cost fabrication method for SACNT/PI composite, which shows improved properties and great potential for a wide range of applications. Several thermo-related applications such as serving as a heater and an actuator have been demonstrated in this paper. Commercial PI film heater is usually made by copper foil or nickel-chromium alloy plate electrodes embedded in PI film. Compared with it, SACNT/PI composite film heater we develop has the advantages of low cost, simple fabrication process, fitting more closely together with heated objects, being freely cut after being fabricated and other special functions such as high-temperature fast response, controllability under PID unit, addressability and RF permeability. Besides, SACNT/PI composite film can work as actuators, showing its potential application in soft robots. It is expected that more and more applications of SACNT/PI composite film will be developed in the future.

## 2. Experimental

### 2.1. Synthesis of Poly(amic acid) (PAA)

2.0024 g of ODA (10 mmol) is placed in a three-neck flask containing 30.68 mL of anhydrous DMAc under nitrogen purge at room temperature. After ODA is completely dissolved in DMAc, 2.1812 g of PMDA (10 mmol) is added in one portion. Thus, the solid content of the solution is ~12%. The mixture is stirred at room temperature under nitrogen purge for 12 h to produce a viscous PAA solution. The viscosity of the resultant PAA estimated from Cone Plate Viscometer is 7046 cp.

### 2.2. SACNT/PI composite preparation

We have used the XPS (ESCALAB 250Xi), Raman (HORIBA Lab-RAM HR) and TEM (Tecnai F20) to characterize the SACNT. The Raman result (Fig. 1a) shows the typical line shape of CNT [29]. The XPS results (Fig. 1b) depict the existence of  $sp^2$  (C=C, ~284.7 eV) and  $sp^3$  hybridization (C–C, ~285.4 eV) bonding from the carbon peaks of SACNT films [30]. The TEM image (Fig. 1c) shows the CNTs are multi-walled with a diameter of around 10 nm. Besides, the tube-diameter distribution of super-aligned arrays is well controlled in the previous work of our group [31]. The facile fabrication process for SACNT/PI composite film is shown in Fig. 1d. SACNT film is directly drawn from as-grown SACNT arrays [25] and placed on a glass substrate. Multiple layers of SACNT film are parallel-stacked or cross-stacked to get an aligned thick CNT film or an uniform CNT mesh respectively. By tuning the number of layers and patterning SACNT by laser, the CNT content and patterned CNT structures in the composite film can be precisely controlled. The monomer solution with ~12% solid content is coated on SACNT films directly, which will gradually penetrate into the SACNT films automatically. Following that, thermal imidization, evaporation of residual solvent and crystallization are achieved in a muffle furnace

at programmed temperature series of 80, 120, 180, 300 and 350 °C for 1 h respectively. Finally, the film is peeled off from the substrate. By controlling the amount, alignment and patterning of SACNT film, different types of SACNT/PI composite films can be fabricated. The advantages of this method include larger CNT content and improved dispersion, as compared with traditional methods. At the same time, it is an easy-operating and low-cost process to make self-dispersed SACNT preforms, which is more environmentally friendly due to reduced chemical treatments and favorable for industrial mass production of SACNT/PI composite film.

### 2.3. Materials characterization

Mechanical properties are measured by a MicroTester (Instron 5848) with a sensor at 100 N and a tensile rate of 2 mm/min. All the samples have the same dimension of 30 mm × 10 mm, and five identical samples are tested for each type. In order to evaluate the electrical conductivity, SACNT/PI composite film is cut into a uniform size of 1 cm × 1 cm with two ends connected to silver electrodes, and the electrical conductivity is averaged from 5 repeated measurements. Thermogravimetric analyzer (TGA, NETZSCH STA449C) is used to investigate the thermal stability of the composite films. Samples are heated from 50 °C to 1000 °C at a rate of 10 K/min in flowing air. The coefficient of thermal expansion (CTE) of PI and CNT film is tested by using TA Q400 thermal analysis system.

## 3. Results and discussions

### 3.1. Morphology and structure characterization

Microscopic morphology and structure of SACNT/PI composite film are characterized by scanning electron microscope (SEM, FEI Nova Nano 450), focused ion beam-scanning electron microscope (FIB-SEM, FEI Helios G4 CX) and atom force microscope (AFM, Seiko SPA 300HV). The surface morphology of SACNT/PI composite film (shown in Fig. 1e) clearly demonstrates that CNTs distribute uniformly on the surface. However, after gold-plating on the surface of sample, CNTs are almost invisible, as shown in Fig. 1f. It can be induced by the fact that the surface of SACNT/PI composite film is very flat, and the CNTs very close to the surface also contribute secondary electron signals resulting in a material contrast [32]. The AFM tests (Fig. 1g–h) indicate that the  $R_a$  (arithmetical mean deviation of the profile) of the surface before and after gold-plating are both around 1 nm. The small surface roughness of the composite film makes it an ideal flexible and flat substrate for electronics. Fig. 1j and k represent the cross-sectional SEM images of composite film which are polished by sandpaper and cut by Ga focused ion beam, respectively. Fig. 1j clearly shows that the film can be divided into two areas, a high CNT content area A and PI area B, which is confirmed by the dividing line in the thickness direction in Fig. 1k. The inset figure in Fig. 1j reveals that CNTs are uniformly buried in PI and good interfacial contact is formed.

### 3.2. Physical property characterization

The tensile test results of SACNT/PI composite film (shown in Fig. 2a–c) indicate that it possesses greater mechanical strength, higher Young's modulus and larger tensile failure compared with pristine PI. The tensile strength of 10 layer and 20 layer samples increases to 85.90 MPa and 117.23 MPa, corresponding to 9.0% and 48.8% improvement compared with pristine PI. The Young's modulus of 10 layer and 20 layer sample increases to 3.07 GPa and 4.40 GPa, corresponding to 26.7% and 80.3% improvement respectively. Most notably, the Young's modulus for 100 layer sample is as

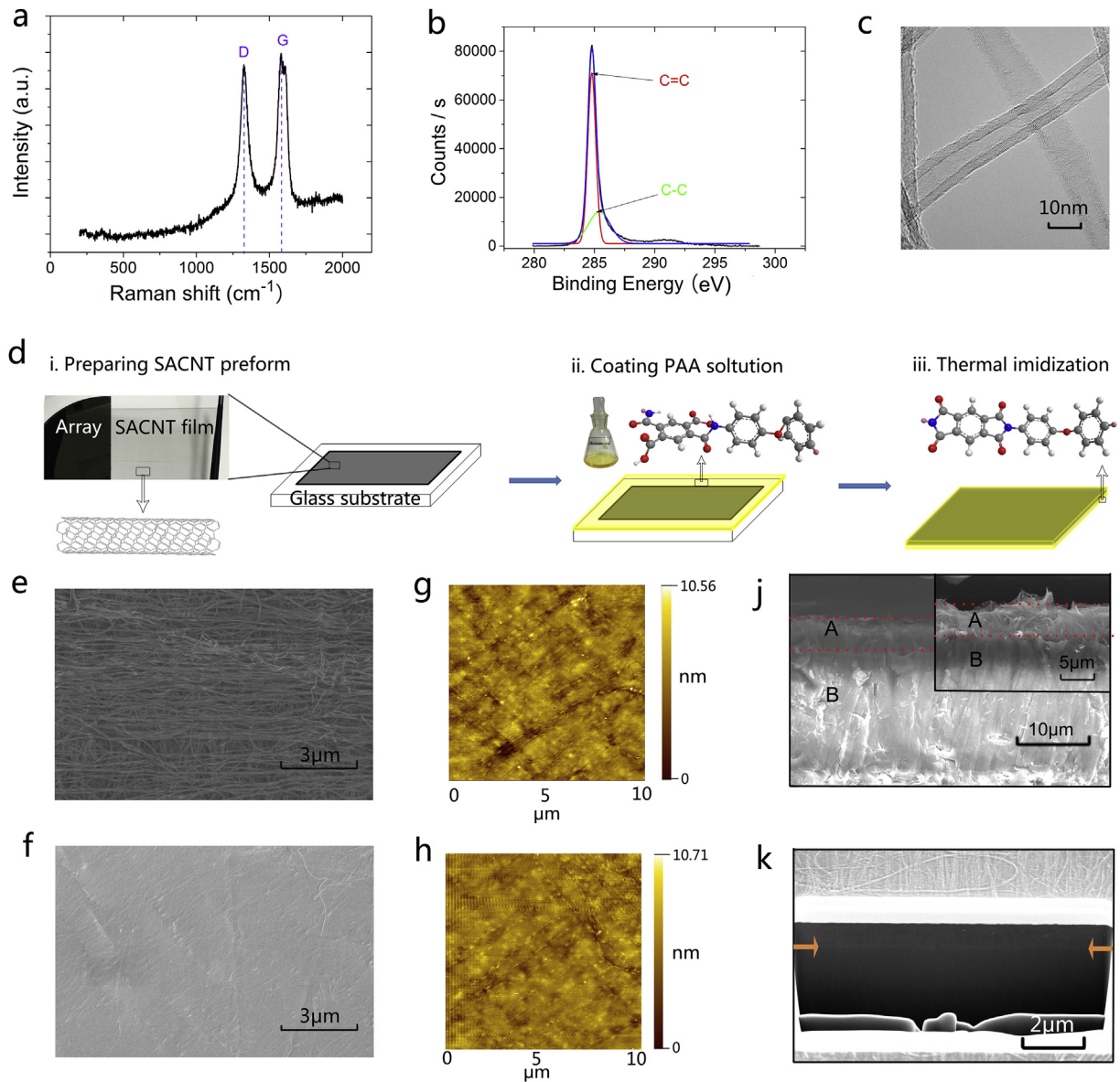


**Fig. 1.** The basic characterization of SACNT film, fabrication process and morphology of SACNT/PI composite film. a-c, The Raman spectrum, XPS spectra and TEM image of SACNT film. d, Schematic illustration of the fabrication process of SACNT/PI composite film. e-f, SEM images of the SACNT/PI composite film surface: e, Original; f, After 3 nm gold-plating. g-h, AFM characterization of SACNT/PI composite film: g, Original; h, After 3 nm gold-plating. j-k, Cross-sectional SEM images of the SACNT/PI composite film: j, The composite film is sandwiched by Si wafers and is polished by sandpaper for SEM, inset: the enlargement of j; k, The composite film is deposited 500 nm Pt and cut by Ga focused ion beam with 30 keV energy for SEM observation, the angle between electron beam and ion beam is  $52^\circ$ . (A colour version of this figure can be viewed online.)

high as 7.41 GPa which is triple that of the pristine PI. The tensile failure of 10 layer and 20 layer sample increases to 8.39% and 10.28%, corresponding to 10.7% and 35.7% improvement compared with pristine PI. Both the tensile strength and tensile failure increase to the maximum for 20 SACNT film layer sample and then decrease with CNT content, while the Young's modulus continuously goes up with the CNT content. According to Ref. [33], the mechanical properties of a composite material depend on the behavior of individual elements and their load transfer across interface. Yu et al. reported that an individual CNT's tensile strength and Young's modulus are 11–63 GPa and 270–950 GPa respectively [34]. The cross-stacked SACNT films form interconnected network, benefiting good load transfer [33]. It is reasonable that the presence of CNTs does contribute to the improved mechanical properties of SACNT/PI composite film. However, since the fracture of film is always initiated from the formation of cracks and the presence of CNT

might increase the probability of crack formation, the tensile strength of the composite film is therefore decreased with too much content of CNT. Since the Young's modulus of CNT is greatly larger than that of PI and the composite has great load transfer, adding more CNTs can help to improve the Young's modulus of composite film. According to our results, the tensile failure of composite film is positively related to tensile strength and negatively related to Young's modulus, leading to the trend with CNT content shown in Fig. 2c. The improved mechanical properties of SACNT/PI composite film make it more durable and stable.

The electrical conductivity of composite films is plotted against the number of CNT layers in Fig. 2d, revealing that SACNT/PI composite film possesses good electrical conductivity even though PI is an insulator. The sheet resistance of pristine one-layer SACNT film is about  $1 \text{ k}\Omega/\text{sq}$  [27], while the sheet resistance of one-layer SACNT/PI composite film is also around  $1 \text{ k}\Omega/\text{sq}$ . Although the

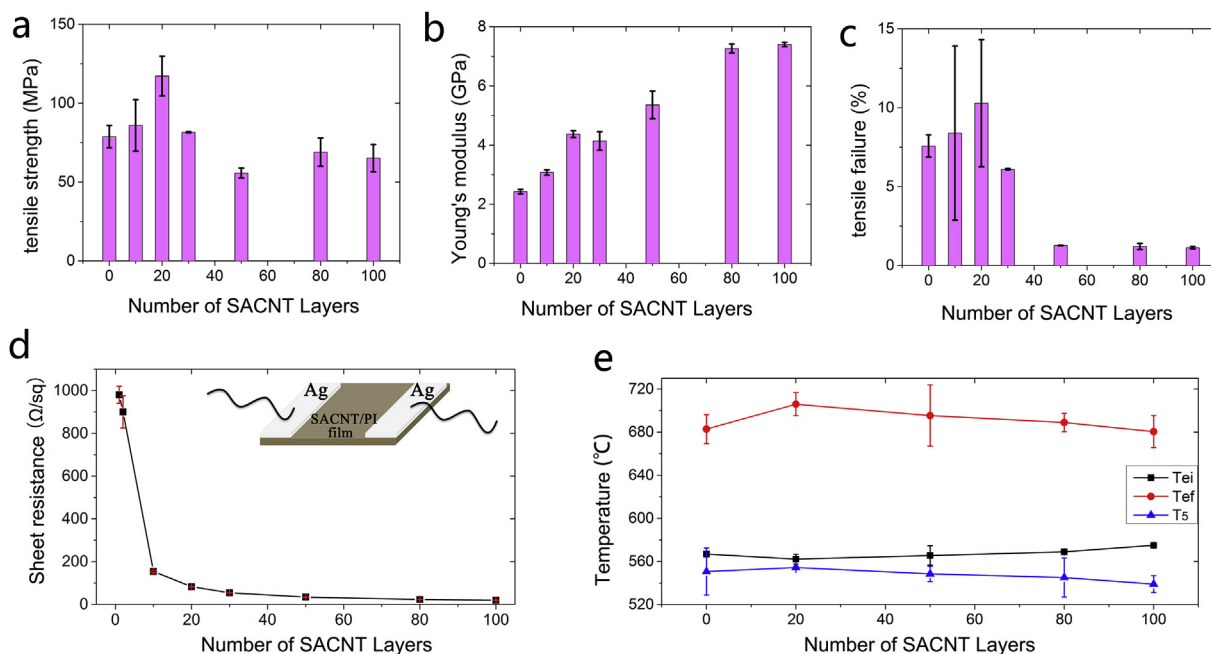


**Fig. 2.** Mechanical, electrical and thermal properties of the SACNT/PI composite film. a–c, The tensile strength, Young's modulus, tensile failure of SACNT/PI composite film at different CNT content; d, The sheet resistance of film at different CNT content, inset: the schematic diagram of measured sample; e, Extrapolated initial decomposition temperature ( $T_{ei}$ ), extrapolated final decomposition temperature ( $T_{ef}$ ), and the temperature of weight loss of 5% ( $T_5$ ) of SACNT/PI composite films at different CNT content via TGA tests. (A colour version of this figure can be viewed online.)

majority of SACNT are embedded in PI (as shown in Fig. 1j), they still can greatly improve the electrical conductivity. A possible reason might be that electrons will tunnel through the very thin PI coating on CNTs. Some CNTs exposing on the surface also attribute the electrical conductivity. The other side of SACNT/PI composite film is almost pure PI, which is an excellent insulator. In general, the electrical conductivity of SACNT/PI composite film increases with CNT content as shown in Fig. 2d. Because the space ratio of one layer SACNT film is about 80%, there are many voids among SACNT films [27]. The CNTs will fill the voids to form a denser electrical conductive network with increasing the number of SACNT layers, leading to a sharp decrease of sheet resistance. However, when the SACNT content is larger than 20 layers, the electrical conductivity of SACNT/PI film grows slowly with the CNT content because enough conductive paths have already been built. The good electrical conductivity of SACNT/PI composite film makes it an ideal conductor for a variety of applications including conductive surfaces that preventing electrostatic charge accumulation.

Thermal properties of the composite films are characterized by using Thermogravimetric analyzer (TGA). The heat stability is characterized by the extrapolated initial decomposition temperature ( $T_{ei}$ ), extrapolated final decomposition temperature ( $T_{ef}$ ), and the temperature at which weight loss reaches 5 wt% ( $T_5$ ). PI is one of the most thermally stable polymers [35,36], and SACNT also exhibits great heat resistance. The TGA test results (shown in Fig. 2e) reveal that the combination of SACNT and PI keeps the high temperature performance of them. The  $T_{ei}$  of pristine PI and SACNT are 566.9 °C and more than 600 °C [37] respectively. The  $T_{ei}$  and  $T_5$  of SACNT/PI composite film reaches up to 562–575 °C and 539–554 °C, indicating great potential in thermal applications.

### 3.3. Thermo-related applications of SACNT/PI composite film

Due to the improved mechanical strength, electrical conductivity, and heat resistance, SACNT/PI composite film can be widely

used in thermo-related applications such as multifunctional heaters and actuators, with the merits of very thin and truly flexible. Especially, the patterned SACNT structures on composite film can act as electrodes. As shown in Fig. 3a–b, the SACNT/PI composite film can be easily heated by an electric current. The temperature–time curves of SACNT/PI composite film at different pulsed voltages (in Fig. 3c) clearly show a very fast high-temperature thermal response and a relatively constant temperature under a constant voltage. As shown in Fig. 3d, the response time from room temperature to the steady temperature ranges from 1.3 s to 4.9 s, while the time for cooling down to room temperature is less than 2.2 s. The heating rate and cooling rate range from 3.3 °C/s to 118.0 °C/s and 9.9 °C/s to 116.0 °C/s respectively, both show a roughly positive correlation with the steady temperature. When being controlled via a PID control unit (Fig. 3e), the SACNT/PI composite film can keep its temperature stable and the standard deviation of the controlled temperature is less than 5.2 °C (Fig. 3f–g). These results indicate that the SACNT/PI composite film is capable of being used as a heater which can response quickly to a preset temperature.

Fig. 3h also shows that SACNT/PI composite film can be used as a flexible heater, boiling 30 ml water from 20.7 °C within 5.3 min, at a power consumption of 40 W. The energy efficiency is about 78% without any measures to prevent heat dissipation. Because of its small thickness, the film can be attached tightly to surfaces simply, which also gives rise to good temperature uniformity. Unlike conventional heater which is made from heating wire, the SACNT/PI thin film heater can be penetrated through by RF field. As shown in Fig. 3i, an inductively coupled plasma (ICP) was generated by using a RF coil. A SACNT/PI thin film heater working at 200.7 °C is inserted between the coil and the quartz tube, which do not affect the formation of the ICP. This offers great convenience for applications which require both ICP and high temperature simultaneously.

Another big advantage over the conventional heater is that the SACNT/PI thin film heater can be patterned simply by laser cutting

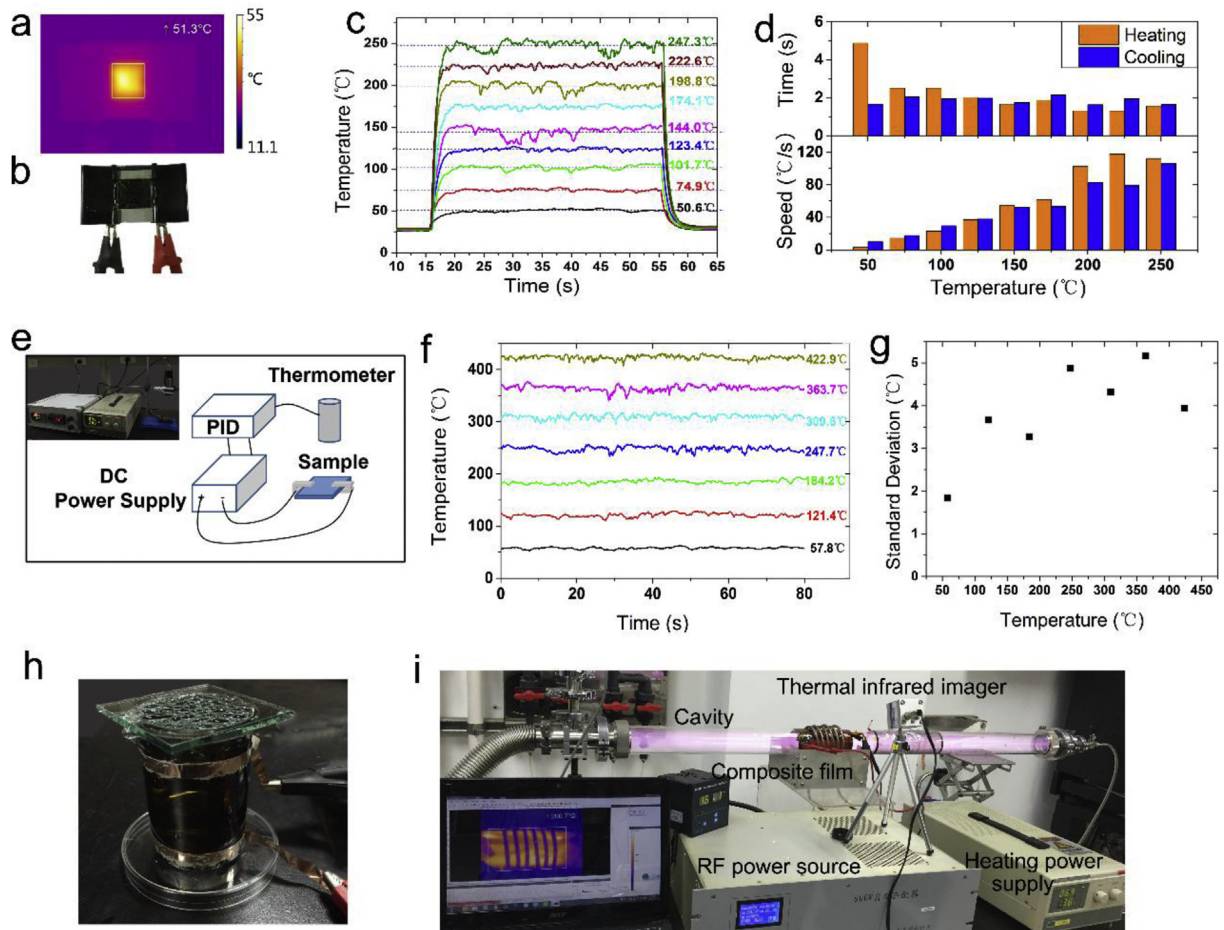


**Fig. 3.** SACNT/PI composite film as fast thermal response, temperature controllable, flexible and RF permeable heater. a, The infrared image of SACNT/PI composite film heated around 50 °C; b, The photo of SACNT/PI film heater; c, The temperature-time curves of SACNT/PI film heater under different heating voltages; d, The response time and speed of SACNT/PI film heater during heating and cooling; e, The diagram of PID temperature control system, inset: the image of PID temperature control system; f, The temperature-time curves of SACNT/PI film heater under a PID temperature control; g, The temperature fluctuation by PID temperature control; h, The photo of a flexible SACNT/PI film heater attached to glass cup to boil the water; i, Experimental installation of the inductively coupled plasma (ICP), in which case RF field can penetrate through SACNT/PI heater. (A colour version of this figure can be viewed online.)

[28], which enables an addressable heater array as shown in Fig. 4a. SACNT film is first cut into “L” shape on substrate forming a  $16 \times 16$  patterned array, then the patterned SACNT film is made into the SACNT/PI composite film. The row and column electrodes and the electrical insulation layer are screened-printed with conductive and insulating pastes, respectively. Fig. 4b shows the IR images of an individual pixel and a  $4 \times 4$  array under different applied voltage. The temperature of the pixel can be controlled by the power supply (see in Fig. 4b(i-ii) and supporting movie 1). The addressable heater can perfectly work in case of arbitrary deformation (see in Fig. 4b(iii-iv) and supporting movie 2). The I–V curves of the addressable heater shows an Ohmic-conductive behavior (Fig. 4c), and the experimental data of the selected pixel's and  $4 \times 4$  array's temperature versus power can be well fitted to a straight line (red and green line in Fig. 4d). This offers the feasibility of precise temperature control. Besides, the addressable heater exhibits a fast response to the voltage owing to the ultra-small heat capacity per unit area. The response time and heating/cooling speeds at different applied voltage are shown in Fig. 4e–f. The heating response time is decreasing with voltage (1.6 s at 20 V), while the cooling response time is almost constant (2–3 s). Both the heating and cooling speed increase with voltage.

Supplementary video related to this article can be found at

<https://doi.org/10.1016/j.carbon.2018.08.011>

In SEM images (Fig. 1j–k), we can see that the composite film can be divided into two part in the thickness direction. One is the area A with a high content of oriented CNTs and exhibits great electrical conductivity, the other is the area B which consists of PI. In the temperature ranging from room temperature to about 350 °C, the measured coefficient of thermal expansion (CTE) of PI and CNT film are 46 ppm/°C and  $-0.7$  ppm/°C respectively. The notable difference in CTE between SACNT and PI as well as the fast thermal response imply that the SACNT/PI composite film might act as a fast-response flexible thermal actuator. When applying a voltage, the electrical conductive composite film can be heated. Because of the small thickness of the composite film, the heat can spread quickly so that the composite film has a relatively uniform heat distribution in the thickness direction. The different CTE of two sides of the composite film results in different deformation, leading to the mechanical movement. The actuator can be easily shaped into different 3D structures like a flower, grass, gripper and so on. Fig. 5 and supporting movie 3–4 show a flower and a grass actuator made from SACNT/PI composite films, which are obviously deformed when the voltage is switched on. The deformation can recover rapidly after switching off the heating. Besides, the SACNT/PI gripper of 20 mg can easily move an object of 51 mg, as shown in

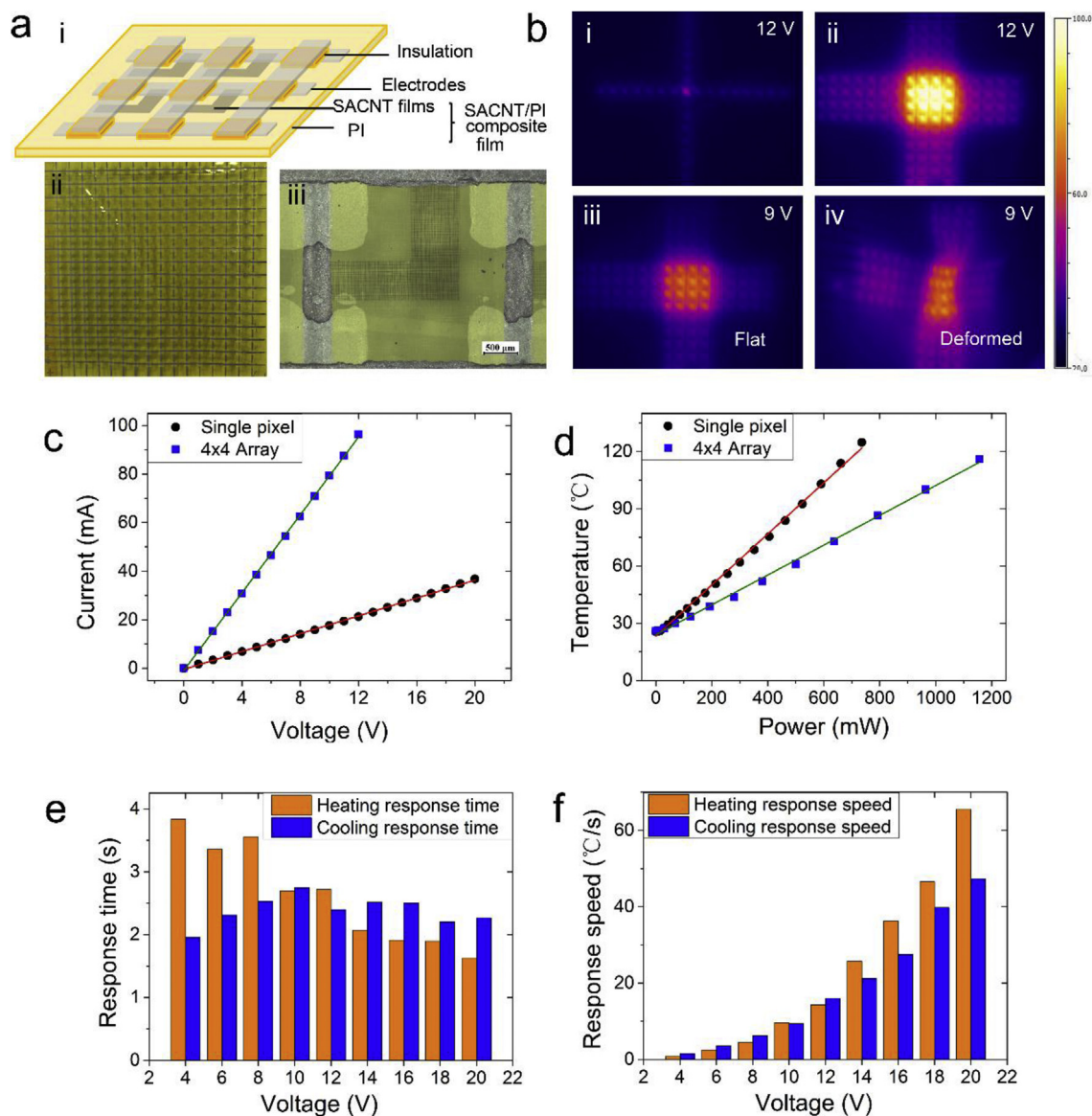


**Fig. 4.** Characterization and performance of flexible addressable SACNT/PI film heater array. a: i, Schematic illustration, ii, photo image, and iii, microscope image at 20 $\times$  of SACNT/PI film addressable heater array; b, The infrared images of heater array: i, individual pixel at 12 V, ii, 4  $\times$  4 array at 12 V, iii, flat 4  $\times$  4 array, and iv, deformed 4  $\times$  4 array; c, I-V curves of the addressable heater (the red line and green line represent linearly fitted data); d, Temperature-power curves of the addressable heater (the red line and green line represent linearly fitted data); e, The response time of heater during heating and cooling; f, The response speed of heater during heating and cooling. (A colour version of this figure can be viewed online.)

Fig. 5c and supporting movie 5-6, indicating its potential application in soft robots.

Supplementary video related to this article can be found at <https://doi.org/10.1016/j.carbon.2018.08.011>.

So far we have demonstrated the applications such as flexible addressable heaters and actuators. However, the SACNT/PI composite film has great potential in even more diverse applications such as flexible conductive substrates for electronics integration and energy storage device, electrostatic shielding materials, RFID and so on. The heater can be used in heating biological and medical equipment, heating satellite and spacecraft component to prevent failure by low temperature, maintaining constant temperature of optoelectronic devices and outdoor electronic equipment and so on. Compared with the commercial PI film heater, SACNT/PI film heater do not need additional electrodes made by copper foil or nickel - chromium alloy plate, being much cheaper and more easily

to be fabricated. The SACNT/PI film can be patterned easily by low-power laser without molds, and easily to be tailored to the desired shape. It can be attached to the object more conveniently for its tiny thickness of  $\sim 10$   $\mu$ m. Thanks to the ultra-thin thickness, flexibility, heat uniformity, fast high-temperature thermal response, controllability under PID unit, addressability, and tunable electromagnetic transmittance, more and more applications of the SACNT/PI composite film will be developed in the near future.

#### 4. Conclusion

In this paper, SACNT/PI composite films with high content of well-dispersed and orientation-controlled patterned CNT structures are obtained via a simple approach without prior CNT dispersion. Not only can the self-dispersed and self-supported SACNT films simplify the preparing of composite film, but also

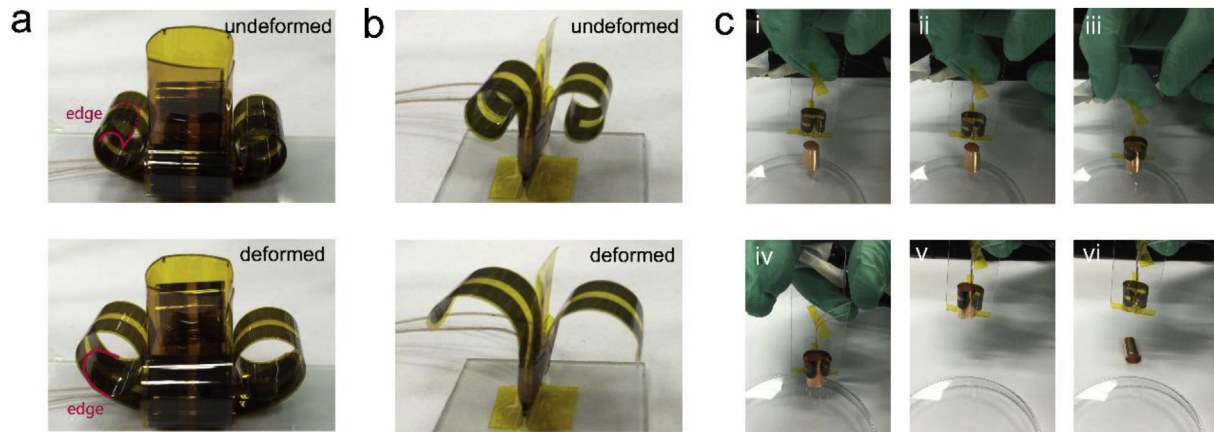


**Fig. 5.** Thermomechanical behavior of the actuator based on SACNT/PI composite film. The driving power are 5.6 W(a), 2.7 W(b) and 1.2 W(c), respectively. a-b, The composite film can be shaped into the 3D structures of flower as well as grass, and it is deformed when the voltage is switched on; c, The gripper (weighted 20 mg) made by composite film can move an object weighted 51 mg: i, Original state; ii, The gripper stretches when the voltage is switched on; iii, Move the gripper to plug the object into the gripper; iv, The object gets stuck by gripper when the voltage is switched off; v, Move the object; vi, The object is released when the voltage is switched on. (A colour version of this figure can be viewed online.)

they can work as patterned transparent electrically and thermally conductive networks to improve the properties of composite film. The SACNT/PI composite film exhibits improvement in mechanical strength, Young's modulus, electrical conductivity compared with pristine PI, and shows good thermal stability. Several thermo-related applications based on these properties have been demonstrated, such as a flexible, stable, addressable, electromagnetic wave permeable, and high-temperature fast-response heater which is much superior to commercial PI film heater as well as a thermo-mechanical actuator. Our work provides a great avenue to fabricate low-cost and high-performance multifunctional materials based on self-dispersed nanomaterials, especially a wide variety of SACNT/polymer composite films, in a simple method which is favorable for industrial mass production. Furthermore, it is expected that the SACNT/polymer composite film will play important roles in more and more applications, such as electrostatic shielding materials, flexible/wearable devices, RFID and so on.

### Acknowledgements

This work is financially supported by the NSFC (51727805, 51672152, 51472141), the National Basic Research Program of China (2014CB643604), The National Key Research and Development Program of China (2017YFA0205800). This work is supported in part by the Beijing Advanced Innovation Center for Future Chip (ICFC).

### References

- [1] S. Iijima, Helical microtubules of graphitic carbon, *Nature* 354 (6348) (1991) 56–58.
- [2] R. Andrews, M.C. Weisenberger, Carbon nanotube polymer composites, *Curr. Opin. Solid State Mater. Sci.* 8 (1) (2004) 31–37.
- [3] Y. Zeng, P. Liu, J. Du, L. Zhao, P.M. Ajayan, H.-M. Cheng, Increasing the electrical conductivity of carbon nanotube/polymer composites by using weak nanotube–polymer interactions, *Carbon* 48 (12) (2010), 3551–3558. doi:10.1016/j.carbon.2010.08.023.
- [4] P. Chunzheng, C. Chilan, T. Haobin, Z. Jianguo, Mechanical enhancement and crystallization kinetics of polyoxymethylene-based composite film with carbon nanotube, *J. Thermoplast. Compos. Mater.* 30 (5) (2017), 599–607. doi:10.1080/0892-7057.
- [5] M.H. Al-Saleh, U. Sundararaj, Electromagnetic interference shielding mechanisms of CNT/polymer composites, *Carbon* 47 (7) (2009) 1738–1746.
- [6] N. Ghatge, N. Maldar, Polyimides from dianhydride and diamine: structure property relations by thermogravimetric analysis (TGA), *Polymer* 25 (9) (1984) 1353–1356.
- [7] K.L. Mittal, *Polyimides: Synthesis, Characterization, and Applications*, Springer Science & Business Media, 2013.
- [8] P.Y. Apel, I.V. Blonskaya, V.R. Oganessian, O.L. Orelovitch, C. Trautmann, Morphology of latent and etched heavy ion tracks in radiation resistant polymers polyimide and poly(ethylene naphthalate), *Nucl. Instrum. Methods Phys. Res. Sect. B Beam Interact. Mater. Atoms* 185 (1) (2001) 216–221.
- [9] D. Wilson, H.D. Stenzenberger, P.M. Hergenrother, *Polyimides—chemistry and Application*, Blackie, Glasgow, London, 1990.
- [10] D. Thuau, V. Koutsos, R. Cheung, Electrical and mechanical properties of carbon nanotube–polyimide composites, *J. Vac. Sci. Technol. B: Microelectron. Nanometer Struct.* 27 (6) (2009) 3139.
- [11] B. Zhu, S. Xie, Z. Xu, Y. Xu, Preparation and properties of the polyimide/multi-walled carbon nanotubes (MWNTs) nanocomposites, *Compos. Sci. Technol.* 66 (3–4) (2006) 548–554.
- [12] X. Jiang, Y. Bin, M. Matsuo, Electrical and mechanical properties of polyimide–carbon nanotubes composites fabricated by in situ polymerization, *Polymer* 46 (18) (2005) 7418–7424.
- [13] D. Hill, Y. Lin, L. Qu, A. Kitaygorodskiy, J.W. Connell, L.F. Allard, Y.-P. Sun, Functionalization of carbon nanotubes with derivatized polyimide, *Macromolecules* 38 (18) (2005) 7670–7675.
- [14] Z. Spitalsky, D. Tasis, K. Papagelis, C. Galiotis, Carbon nanotube–polymer composites: chemistry, processing, mechanical and electrical properties, *Prog. Polym. Sci.* 35 (3) (2010) 357–401.
- [15] L. Vaisman, H.D. Wagner, G. Marom, The role of surfactants in dispersion of carbon nanotubes, *Adv. Colloid Interface Sci.* 128–130 (Supplement C) (2006) 37–46.
- [16] L. Nayak, M. Rahaman, A. Aldabhi, T. Kumar Chaki, D. Khastgir, Polyimide-carbon nanotubes nanocomposites: electrical conduction behavior under cryogenic condition, *Polym. Eng. Sci.* 57 (3) (2017) 291–298.
- [17] E.J. Siochi, D.C. Working, C. Park, P.T. Lillehei, J.H. Rouse, C.C. Topping, A.R. Bhattacharyya, S. Kumar, Melt processing of SWCNT-polyimide nanocomposite fibers, *Compos. B Eng.* 35 (5) (2004) 439–446.
- [18] Z. Jin, K.P. Pramoda, S.H. Goh, G. Xu, Poly(vinylidene fluoride)-assisted melt-blending of multi-walled carbon nanotube/poly(methyl methacrylate) composites, *Mater. Res. Bull.* 37 (2) (2002) 271–278.
- [19] J. Gou, Single-walled nanotube bucky paper and nanocomposite, *Polym. Int.* 55 (11) (2006) 1283–1288.
- [20] Z. Wang, Z. Liang, B. Wang, C. Zhang, L. Kramer, Processing and property investigation of single-walled carbon nanotube (SWNT) buckypaper/epoxy resin matrix nanocomposites, *Compos. Appl. Sci. Manuf.* 35 (10) (2004) 1225–1232.
- [21] K. Wang, Y.-H. Chang, C. Zhang, B. Wang, Conductive-on-demand: tailorable polyimide/carbon nanotube nanocomposite thin film by dual-material aerosol jet printing, *Carbon* 98 (2016) 397–403.
- [22] Q. Li, Q.-M. Wang, Inkjet Printing of Carbon Nanotube-polyimide Nanocomposite Strain Sensor, *American Society of Mechanical Engineers*, 2016. V010T13A025-V010T13A025.
- [23] W. Fan, L. Zuo, Y. Zhang, Y. Chen, T. Liu, Mechanically strong polyimide/carbon nanotube composite aerogels with controllable porous structure, *Compos. Sci. Technol.* 156 (2018) 186–191.
- [24] D. Hu, Y. Xing, M. Chen, B. Gu, B. Sun, Q. Li, Ultrastrong and excellent dynamic mechanical properties of carbon nanotube composites, *Compos. Sci. Technol.* 141 (2017) 137–144.
- [25] K. Jiang, Q. Li, S. Fan, Spinning continuous carbon nanotube yarns, *Nature* 419 (6909) (2002).
- [26] Q. Cheng, J. Wang, K. Jiang, Q. Li, S. Fan, Fabrication and properties of aligned

- multiwalled carbon nanotube-reinforced epoxy composites, *J. Mater. Res.* 23 (11) (2011) 2975–2983.
- [27] C. Feng, K. Liu, J.S. Wu, L. Liu, J.S. Cheng, Y. Zhang, Y. Sun, Q. Li, S. Fan, K. Jiang, Flexible, stretchable, transparent conducting films made from superaligned carbon nanotubes, *Adv. Funct. Mater.* 20 (6) (2010), 885–891 %@ 1616-3028.
- [28] P. Liu, L. Liu, Y. Wei, K. Liu, Z. Chen, K. Jiang, Q. Li, S. Fan, Fast high-temperature response of carbon nanotube film and its application as an incandescent display, *Adv. Mater.* 21 (35) (2009) 3563–3566.
- [29] R. Koizumi, A.H.C. Hart, G. Brunetto, S. Bhowmick, P.S. Owuor, J.T. Hamel, A.X. Gentles, S. Ozden, J. Lou, R. Vajtai, S.A.S. Asif, D.S. Galvão, C.S. Tiwary, P.M. Ajayan, Mechano-chemical stabilization of three-dimensional carbon nanotube aggregates, *Carbon* 110 (2016) 27–33.
- [30] T.I.T. Okpalugo, P. Papakonstantinou, H. Murphy, J. McLaughlin, N.M.D. Brown, High resolution XPS characterization of chemical functionalised MWCNTs and SWCNTs, *Carbon* 43 (1) (2005) 153–161.
- [31] K. Liu, Y. Sun, L. Chen, C. Feng, X. Feng, K. Jiang, Y. Zhao, S. Fan, Controlled growth of super-aligned carbon nanotube arrays for spinning continuous unidirectional sheets with tunable physical properties, *Nano Lett.* 8 (2) (2008), 700–705 %@ 1530-6984.
- [32] D. Li, J. Zhang, Y. He, Y. Qin, Y. Wei, P. Liu, L. Zhang, J. Wang, Q. Li, S. Fan, K. Jiang, Scanning electron microscopy imaging of single-walled carbon nanotubes on substrates, *Nano Res.* 10 (5) (2017) 1804–1818.
- [33] P.S. Owuor, Y. Yang, T. Kaji, R. Koizumi, S. Ozden, R. Vajtai, J. Lou, E.S. Penev, B.I. Yakobson, C.S. Tiwary, P.M. Ajayan, Enhancing mechanical properties of nanocomposites using interconnected carbon nanotubes (iCNT) as reinforcement, *Adv. Eng. Mater.* 19 (2) (2017) 1600499.
- [34] M.-F. Yu, O. Lourie, M.J. Dyer, K. Moloni, T.F. Kelly, R.S. Ruoff, Strength and breaking mechanism of multiwalled carbon nanotubes under tensile load, *Science* 287 (5453) (2000) 637–640.
- [35] E. Mazoniene, J. Bendoraitiene, L. Peciulyte, S. Diliunas, A. Zemaitaitis, (Co) polyimides from commonly used monomers, and their nanocomposites, *Prog. Solid State Chem.* 34 (2–4) (2006) 201–211.
- [36] B.P. Singh, D. Singh, R.B. Mathur, T.L. Dhimi, Influence of surface modified MWCNTs on the mechanical, electrical and thermal properties of polyimide nanocomposites, *Nanoscale Res. Lett.* 3 (11) (2008) 444–453.
- [37] K. Liu, Y. Sun, L. Chen, C. Feng, X. Feng, K. Jiang, Y. Zhao, S. Fan, Controlled growth of super-aligned carbon nanotube arrays for spinning continuous unidirectional sheets with tunable physical properties, *Nano Lett.* 8 (2) (2008) 700–705.